Rare earth element anomalies in crandallite group minerals from the Schugorsk bauxite deposit, Timan, Russia

Article *in* European Journal of Mineralogy · November 2000

CITATIONS
31

READS
233

3 authors, including:

Christopher J Stanley
Natural History Museum, London
247 PUBLICATIONS **2,320** CITATIONS

SEE PROFILE

Eur. J. Mineral.
2000, **12**, 1229-1243

Rare earth element anomalies in crandallite group minerals from the Schugorsk bauxite deposit, Timan, Russia

LEONID E. MORDBERG[1,2,3], CHRIS J. STANLEY[2] and KLAUS GERMANN[1]

[1]Technische Universität Berlin, Lagerstättenforschung, Sekr. BH4, Ernst-Reuter-Platz 1, 10587 Berlin, Germany. – e-mail: leo10932@mailszrz.zrz.tu-berlin.de
[2]The Natural History Museum, Cromwell Road London UK, SW7 5BD
[3]Russian Research Geological Institute (BSEGEI), Sredny pr. 74, St. Petersburg 199106, Russia

Abstract: Crandallite group minerals from the Devonian bauxite deposit of Schugorsk, Timan, Russia, were studied by electron microprobe. Special attention was given to the distribution of the rare earth elements (REE). Of the A-site cations, essential are (oxides in wt.%) Ca (0.2 - 7.9), Sr (0.4 - 5.9), Ba (0.1 - 5.1), Pb (0.01 - 8.4), Y (to 2.4) and REE (to 21.6). Bi (A-site), Ga (B-site) and V (X-site) occur in trace amounts. Two main types of REE distribution in crandallite group minerals are distinguished. The first shows a clear negative Ce anomaly and partially depleted Pr; crandallite group minerals of this type formed under strong oxidising conditions (positive Eh and neutral to slightly alkaline pH values) and lost Ce due to its oxidation to Ce^{4+} and accumulation in other minerals such as anatase. The second type displays a positive Sm anomaly and a negative Pr anomaly. Individual crandallite group crystals belonging to this type, 1 - 40 μm in size, show a clear compositional zoning: the core is enriched in Ca, while the rim is enriched in S, Sr, Pb and the REE. This crandallite formed under reducing conditions related to stripping of Fe from the weathering profile. The presence of Sm^{2+} in the crandallite lattice is proposed, and the role of organic material in its reduction is discussed. A Pr anomaly was inherited from the parent rock. A comparison of REE distribution in crandallite group minerals from different weathering profiles suggests that these minerals can be used to distinguish conditions of weathering.

Key-words: bauxite, laterite, weathering, crandallite, goyazite, svanbergite, plumbogummite, hinsdallite, florencite, Rare Earth Elements.

Introduction

Minerals of the crandallite group are known in both lateritic profiles and karst bauxite deposits. Crandallite itself $CaAl_3(PO_3O_{1/2}(OH)_{1/2})_2(OH)_6$ (Blount, 1974) has been recorded in karst bauxite deposits of Hungary, Pacific islands and Jamaica (Bárdossy, 1982). It is also a principal mineral of lateritic profiles over P-rich rocks in the Eastern Amazon Region where it was found in association with other aluminous phosphates such as augelite, variscite, wavellite *etc.* (Schwab *et al.*, 1983). Bushinsky (1975) drew attention to a typical association of P, Sr and S in bauxite profiles. Svanbergite $SrAl_3(PO_4)(SO_4)(OH)_6$ has been recorded in the Tikhvinsk deposit (Ansheles & Vlodavets, 1927), in a few occurrences of the N Urals (Lukanina, 1959; Beneslavsky, 1974), among bauxitic clays of Portugal (Gomes, 1968) and in lateritic bauxite profiles of Kursk Magnetic Anomaly (Bulgakova, 1967; Makarov, 1967); it is an essential mineral of the Zaostrovsk bauxite-phosphorite occurrence, as well as crandallite (Mordberg, 1999). REE-bearing crandallites, including florencite $REEAl_3(PO_4)_2(OH)_6$, are also frequently observed in weathering profiles. They form during weathering and this makes them important as indicators of the conditions of bauxite and laterite formation.

As some of the REE such as Ce and Eu are quite sensitive to changes in Eh and dependent on

0935-1221/2000/0012-1229 $ 3.75

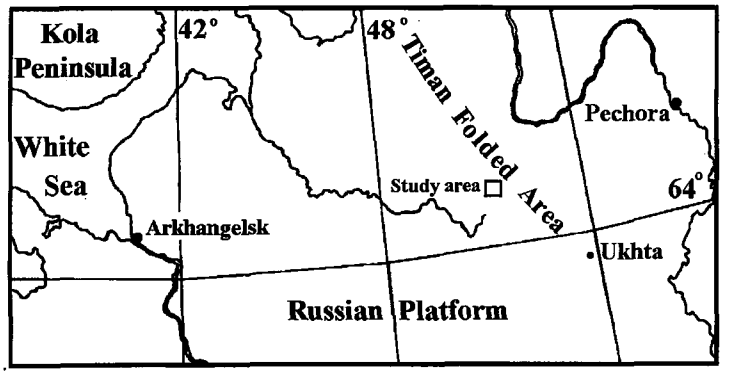

Fig. 1. Location of the study area.

pH and T, the distribution of the REE in crandallite group minerals can be used in the determination of the exact conditions of weathering. A few published analyses of crandallites from different weathering profiles show that the distribution of the REE may be different. Thus, chemical analyses of florencite from laterite over carbonatite in Siberia (Slukin *et al.*, 1989) showed strong enrichment of light REE (LREE) with the absence of anomalous distribution of any element. Apatite-derived crandallites from the weathering profile over phosphorites in Lam-Lam, Senegal (Bonnot-Courtois & Flicoteaux, 1989), are also enriched in LREE, but display a slight positive Sm anomaly, which needs explanation. An analysis of Nd-goyazite from the Vlasenica bauxite deposit of karst origin in Yugoslavia (Maksimović & Panto, 1985) demonstrates a negative Ce anomaly indicating oxidising conditions of bauxite formation. However, recent study (Mordberg *et al.*, submitted) shows, that in spite of the very small size of crandallite grains from bauxite (<50 μm), elements demonstrate a clear zonal distribution with a wide range of compositions even within the smallest crystals. Therefore, chemical analyses of individual grains or a single microprobe analysis cannot give a representative indication of REE distribution patterns and crandallite formation conditions. Thus, a statistically significant number of microprobe analyses is important for the solution of the problem. The present study used crandallite group minerals from the Devonian Schugorsk bauxite deposit, which have inherited their content of the REE from the parent rock.

Geological setting

Bauxite deposits of the Middle Timan are located in the North of European Russia, between the NE edge of the Russian Plate and the Pechorsk Depression (Fig. 1). The geology of the bauxite region has been given in detail by Likhachev (1993) and Mordberg (1996, 1997). Devonian bauxite deposits located within the Chetlass orogenic structure occur on folded, mostly carbonate strata of the Riphean. Deposits of both lateritic and karstic types are found. The overlying rocks are Upper Devonian volcanogenic and sedimentary sequences; in some instances the bauxite profile is covered directly by Late Devonian trap basalt.

The Schugorsk bauxite deposit, the largest in the region, was formed over Precambrian alkali metasomatic silicate-carbonate rock (Fig. 2). Rock-forming minerals of the metasomatite are dolomite and microcline. Calcite, orthoclase, plagioclase, aegirine, riebeckite, biotite and sericite are also present in various amounts. The weathered profile attains a total depth here of 100-120 m, and the main ore-forming minerals are boehmite, kaolinite and hematite with nearly monomineralic white boehmitic bauxites being widespread within the deposit. The ratio of carbonate and silicate minerals in the parent rock varies broadly with an average about 1:1. Due to this heterogeneity, the deposit cannot be referred to either the lateritic or the karstic type.

REE mineralogy

The main carriers of REE in the parent rock are monazite and xenotime. Another REE-rich mineral, bastnaesite-(Ce) or cerianite, was recorded in a few cases. Small amounts of the REE are found in pyrochlore and minerals such as zircon (HREE) and apatite. An unknown mineral of a composition which fits the ideal formula $Fe^{2+}Th(Si,PO_4)(OH,F)_2$ (Mordberg *et al.*, submitted) also contains the REE Ce, La, Nd, Sm and Gd in amounts less

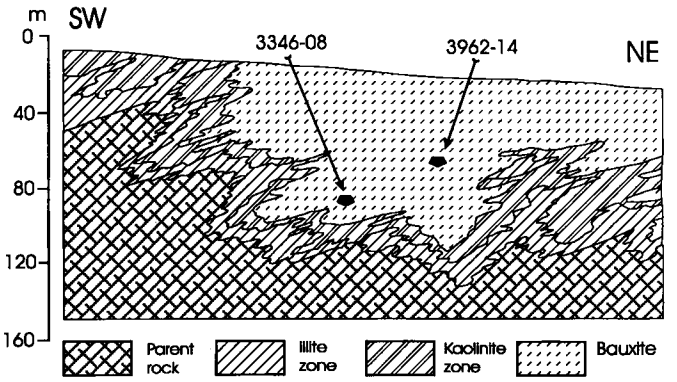

Fig. 2. Geological cross-section of parts of an ore body from the Schugorsk bauxite deposit with the position of the studied samples.

than 1 wt.% each. For the rock-forming minerals, REE should be expected in carbonates and feldspars in amounts comparable with their background for these minerals.

Both monazite and xenotime are typical of the weathering profile. Monazite seems to be the least altered mineral, although its weathering within the profile has been recorded (Likhachev, 1993). Xenotime and zircon altered during profile development forming a metamict solid solution (Mordberg & Spratt, 1998). The REE are preserved in xenotime remains and have accumulated in altered zircon rims (Mordberg *et al.*, submitted). REE-bearing minerals formed during weathering are "leucoxene" (a mixture of anatase and rutile) and those belonging to the crandallite group. The former always contains some Ce, while the latter may represent real florencite. Finally, small amounts of the REE occur in plumbopyrochlore rims, whose cores were inherited from the parent rock.

Material and methods

More than one hundred samples representing the parent rock and all zones of the weathering profile were taken from drill cores. Bulk analyses of the REE (La, Ce, Pr, Nd and Sm) and other trace and major elements were obtained by XRF following the methods described by Krumb (1998) at Technical University of Berlin. Crandallite mineralisation was studied on polished sections of two samples enriched in P and REE by electron microprobe. Their position is shown on Fig. 2. The contents of chemical elements in the minerals were determined using a wavelength-dispersive (WD) electron probe microanalyser (Cameca SX50) at the Natural History Museum, London. International standards were used for calibration of each element. The analytical conditions used were 15 kV and 20 nA with counting times of 20 s for Ca, P, Fe and Al, 30 s for La, Ce, Pb, Ba and 50s for Y, Pr, Nd, Sm, Dy, Er and Yb. The detailed description of determination of the REE by electron microprobe is given by Williams (1996). Elemental X-ray maps were obtained using the following conditions: 15 kV, 100 nA and 200 μS per point.

Results

Although selective weathering of heterogenous parent rock led to the formation of a rather complicated profile (Fig. 2), different mineralogical zones can be distinguished. The distribution parameters of major and trace elements within the profile have already been reported (Mordberg *et al.*, submitted). Chemical and mineral compositions of samples from the parent rock and different zones of the profile are also given in Table 1. Of the trace elements, data are given for those predicted to occur in crandallites. Qualitatively (using energy dispersive electron microprobe analysis), crandallites were identified in a few samples, two of which were found to be relatively enriched in REE (3346-08 and 3962-14) and subjected to quantitative electron microprobe analysis.

Crandallite mineralization is finely dispersed throughout the weathering profile. Normally, the crystal size of crandallite group minerals within the studied profile varies from a few μm to 30-40 μm. A characteristic feature of dispersed crandallite mineralization from the studied deposit is its complex composition (Fig. 3): different element contents represent solid solutions between crandallite - woodhouseite (Ca), goyazite - svanbergite

Table 1. Chemical composition of samples from parent rock and weathering profile.

Sample No.	3962-04	3385-01	7277-04	7277-08	10252-15a	3385-35	3346-08	3385-14	3962-14
wt. %	pr	pr	pr	wp	wp	wp	wp	wp	wp
SiO_2	53.91	24.09	30.44	41.77	40.64	1.53	7.92	0.48	0.64
Al_2O_3	17.42	6.76	8.08	32.16	36.20	59.39	65.73	65.24	74.49
Fe_2O_3	13.31	4.67	3.51	9.04	6.36	21.14	0.57	16.15	1.13
MnO	0.03	0.12	0.12	0.05	0.00	0.08	0.00	0.07	0.01
MgO	0.09	3.09	9.85	0.66	0.07	bdl	bdl	bdl	bdl
CaO	0.54	24.44	16.41	0.15	0.08	0.06	0.34	0.07	0.13
Na_2O	bdl	2.94	2.21	bdl	0.00	bdl	bdl	bdl	bdl
K_2O	10.01	1.08	3.78	3.21	0.31	bdl	0.23	bdl	bdl
TiO_2	0.82	0.36	0.45	1.57	1.80	2.85	4.05	4.07	3.78
P_2O_5	0.38	0.07	0.09	0.07	0.17	0.35	1.78	0.43	1.03
SO_3	0.008	nd	nd	nd	0.015	nd	0.206	0.042	0.05
C_{org}	nd	nd	nd	nd	nd	0.012	0.13	<0.01	nd
L.O.I	2.68	26.73	24.77	10.79	13.91	12.36	15.62	13.02	15.33
SUM	99.20	94.35	99.71	99.47	99.56	97.76	96.57	99.57	96.59
ppm									
As	11	3	3	3	19	2	45	33	12
Ba	654	120	351	348	89	77	966	123	359
Bi	14	24	22	15	9	26	64	22	25
Cu	4	bdl	bdl	bdl	10	9	31	47	13
Ga	28	6	10	39	30	74	99	130	146
Pb	21	5	bdl	6	11	617	2295	52	2169
Sc	12	5	12	44	32	64	100	60	218
Sr	43	79	32	18	552	459	3776	925	1456
Th	75	15	64	28	207	102	113	497	288
V	67	23	79	196	252	301	1712	540	304
Y	178	32	19	42	148	88	244	154	293
La	25	8	bdl	49	51	153	191	137	301
Ce	88	23	15	125	143	277	446	580	1874
Pr	3	1	2	10	8	30	34	23	53
Nd	50	8	25	53	64	225	271	106	408
Sm	8	3	4	9	11	26	35	26	80

pr = parent rock; wp = weathering profile; nd = not determined; bdl = below detection limit.

(Sr), plumbogummite - hinsdalite (Pb), florencite (Ce) and other compounds. However, even these small crystals may show a very clear zoning (Fig. 4): of the elements recorded, Ca and Fe occur in the core of a grain, while Ce, Nd and Pb are present in the rim. Relative enrichment of grain rims with Sr and S was also demonstrated (Mordberg *et al.*, submitted). Similar florencite rims around REE-poor cores are typical for diagenetic crandallites from Permian sandstone in Western Australia (Rasmussen, 1996). The relationship between boehmite and late generation crandallite can be seen from Fig. 5.

Some of the microprobe analyses are given in Table 2. Data on REE contents were not converted to oxides, since the oxidation state of some of them is a subject for discussion. The contents of Al and P vary within the range known for these minerals (Nriagu, 1984a). From Table 2, it can be seen that no one point belongs to any end member except point 20, which can be termed florencite due to high contents of the REE. The analyses show small amounts of Ga, which could have substituted for Al. A few additional microprobe analyses of crandallites also showed the presence of Bi (0.15-0.4 wt.%) and V (0.04-0.07 wt.%), which may substitute for Ca and P respectively. The content of As was always below the detection limit. Both Bi and As were recorded in galena related to epigenetic alteration, and an important concentrator of V is 'leucoxene' (Mordberg *et al.*, submitted).

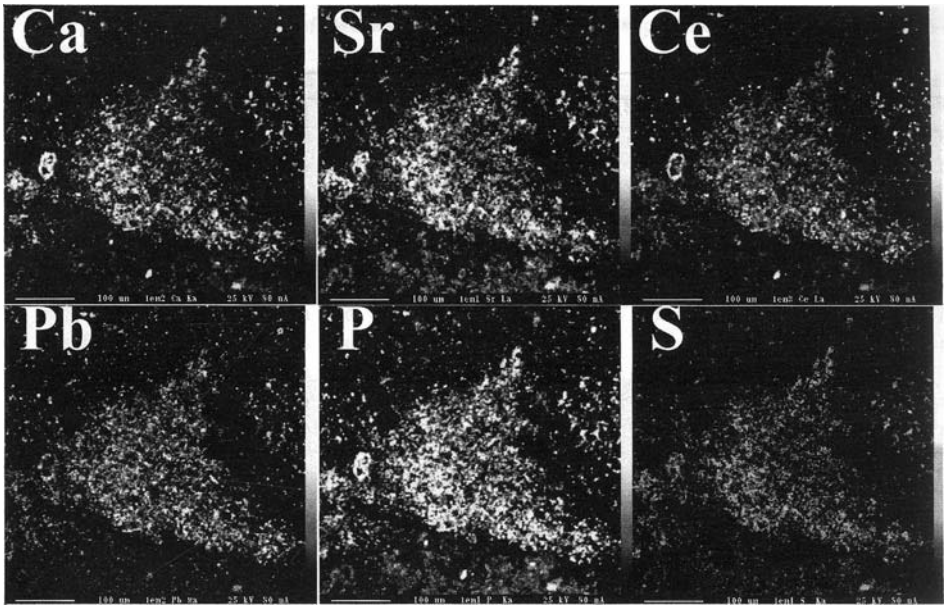

Fig. 3. X-ray maps of elemental distribution in the area of crandallite mineralization: each single crandallite grain has a size of only few μm, but in dense clusters they look like a large crystal. See text for discussion. Bar = 100 μm.

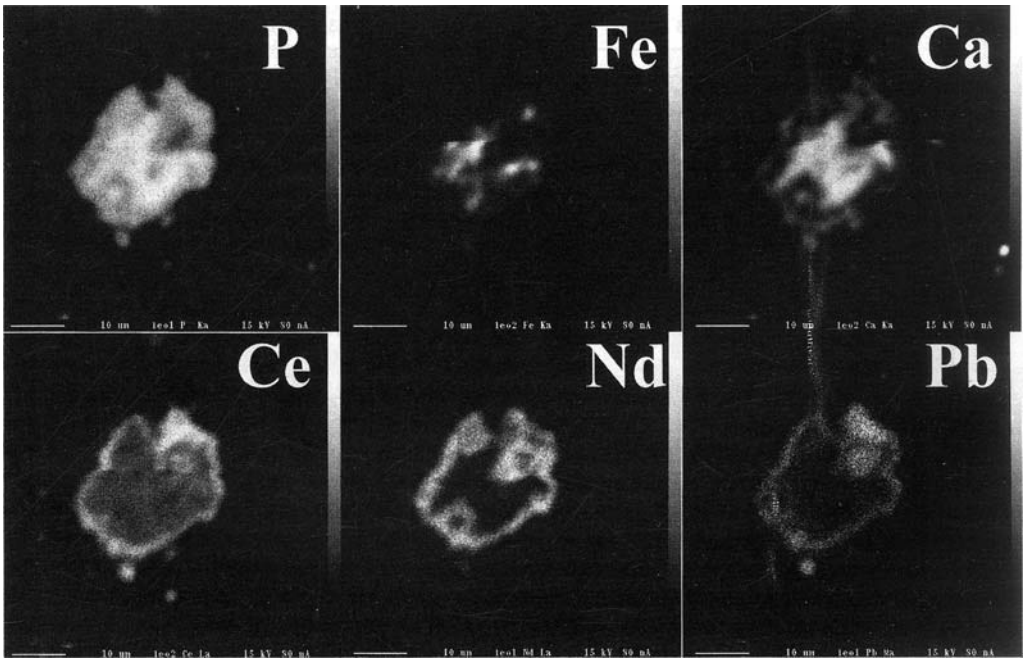

Fig. 4. X-ray maps showing zonal distribution of elements in a single crandallite grain from crandallite mineralization shown in Fig. 3. Bar = 10 μm.

Table 2. Microprobe analyses (wt.%) of crandallite group minerals from bauxite.

	#19	#20	#22	#23	#25	#26	#41	#42	#43	#47	#60
Al_2O_3	34.72	37.00	31.16	34.06	33.17	32.26	34.08	41.59	38.80	36.07	36.09
Fe_2O_3	0.90	0.85	0.88	0.73	0.85	0.33	4.26	1.80	1.37	1.33	1.57
Ga_2O_3	0,03	bdl	0,02	bdl	0,12	0,03	bdl	0,02	bdl	0,01	bdl
P_2O_5	25.81	24.11	20.74	23.22	22.23	21.29	20.93	16.69	19.41	22.25	22.38
SO_3	0.68	0.66	2.20	2.69	2.96	2.46	0.49	0.63	0.43	0.43	0.31
SrO	1.89	1.18	2.96	4.00	4.62	3.37	1.90	1.64	1.89	1.44	0.88
CaO	2.74	2.23	3.56	4.27	3.55	2.69	3.03	2.10	2.58	2.73	4.94
BaO	2.73	1.35	1.60	1.85	1.53	1.40	1.76	1.20	1.85	1.98	2.32
PbO	1.59	2.19	7.54	8.43	7.02	7.56	3.32	3.03	2.11	3.53	0.99
Y_2O_3	2.41	1.50	1.16	0.88	0.84	0.86	0.93	0.98	0.83	0.93	0.50
La	0.26	0.92	0.66	0.59	0.52	0.82	3.24	3.13	2.96	3.36	4.15
Ce	0.44	1.86	1.45	1.59	1.27	1.91	0.94	1.67	1.10	0.92	0.66
Pr	0.06	0.59	0.14	0.01	0.01	0.10	0.42	0.66	0.52	0.69	0.62
Nd	4.15	5.72	1.81	1.82	1.57	1.88	3.55	4.51	2.82	4.28	3.37
Sm	3.04	4.91	0.89	0.79	0.59	0.72	0.73	1.05	0.60	0.81	0.65
Gd	3.05	3.01	0.63	0.66	0.31	0.59	0.54	0.68	0.40	0.61	0.44
Dy	1.13	1.15	0.46	0.36	0.13	0.24	0.12	0.32	0.23	0.25	0.11
Er	0.24	0.07	0.08	0.15	0.20	<0.02	0.04	0.06	0.04	0.07	0.07
Yb	0.05	0.08	0.01	0.08	0.02	0.02	0.03	0.06	0.01	0.19	0.05
$(Y+REE)_2O_3$	16.48	22.60	8.20	7.68	5.99	8.16	12.05	15.03	10.90	13.66	12.19
Total	87.89	92.33	78.96	87.20	82.28	79.57	81.89	83.85	79.39	83.72	81.78

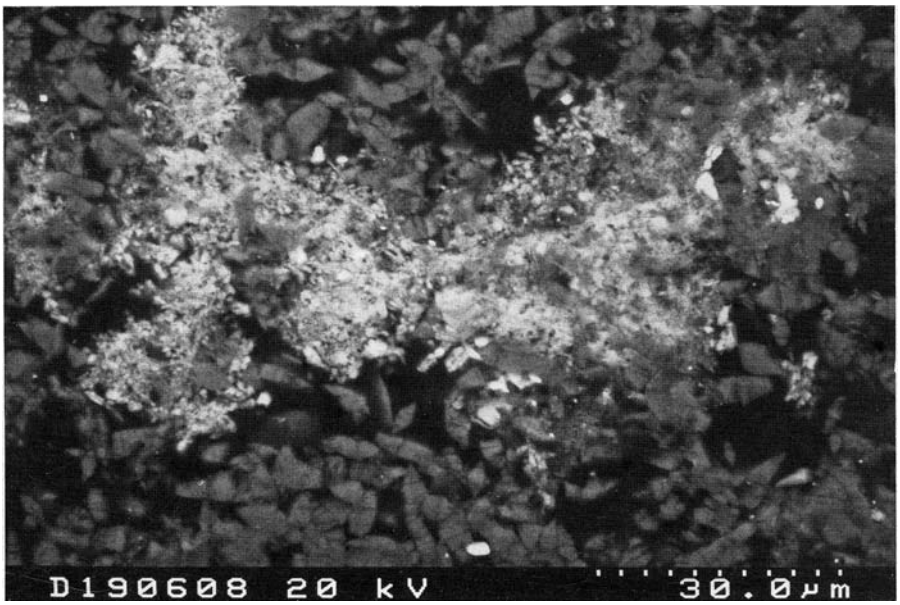

Fig. 5. Backscattered electron image of late generation crandallite among boehmite crystals.

Table 3. Average chemical composition (wt.%) of crandallite-I (19 microprobe analyses) and crandallite-II (23 microprobe analyses).

Crandallite-I	Al_2O_3	P_2O_5	SO_3	Y_2O_3	SrO	CaO	Fe_2O_3	Ga_2O_3	BaO	La_2O_3	Ce_2O_3	Pr_2O_3	Nd_2O_3	Sm_2O_3	Gd_2O_3	Dy_2O_3	Er_2O_3	Yb_2O_3	PbO	Total	$REE_2O_3^*$
Mean	35.48	22.10	0.45	0.97	1.76	3.92	2.38	0.05	1.85	4.03	0.87	0.42	3.44	0.83	0.72	0.34	0.07	0.07	2.12	81.87	11.62
Median	34.11	22.31	0.40	0.97	1.79	4.04	1.92	0.04	1.80	3.87	0.75	0.38	3.07	0.82	0.73	0.36	0.07	0.06	2.13	81.90	11.35
SD	3.17	2.66	0.21	0.20	0.41	1.11	1.64	0.04	0.49	0.65	0.46	0.26	1.00	0.19	0.15	0.12	0.04	0.07	0.89	1.34	1.54
Min.	32.27	16.69	0.16	0.50	0.88	2.10	0.75	0.00	1.20	3.12	0.24	0.10	2.44	0.55	0.46	0.13	0.00	0.00	0.96	79.39	9.71
Max.	41.59	26.76	0.95	1.30	2.44	5.32	6.69	0.12	3.01	5.09	1.96	0.81	5.26	1.22	1.02	0.48	0.13	0.22	3.53	83.85	15.03
Crandallite-II	Al_2O_3	P_2O_5	SO_3	Y_2O_3	SrO	CaO	Fe_2O_3	Ga_2O_3	BaO	La_2O_3	Ce_2O_3	Pr_2O_3	Nd_2O_3	Sm_2O_3	Gd_2O_3	Dy_2O_3	Er_2O_3	Yb_2O_3	PbO	Total	$REE_2O_3^*$
Mean	32.92	24.71	1.87	0.67	3.55	5.10	1.43	0.02	2.42	0.59	1.14	0.02	1.59	0.76	0.61	0.27	0.09	0.03	3.45	81.24	5.65
Median	32.59	25.59	1.88	0.62	3.37	5.16	0.85	0.01	2.53	0.61	1.27	0.00	1.52	0.72	0.62	0.28	0.08	0.02	1.69	81.51	5.52
SD**	2.92	3.88	0.89	0.23	1.43	1.77	1.66	0.03	0.79	0.20	0.57	0.05	0.63	0.26	0.25	0.13	0.07	0.04	3.00	3.55	1.86
Min.	24.60	15.67	0.71	0.31	1.62	1.97	0.33	0.00	1.40	0.28	0.08	0.00	0.00	0.16	0.08	0.02	0.00	0.00	0.41	75.28	1.50
Max.	37.66	32.63	3.49	1.18	6.39	8.39	7.77	0.12	4.64	0.97	2.24	0.17	2.56	1.22	0.96	0.53	0.23	0.10	8.43	88.21	8.20

*Y is included. **SD = Standard Deviation

Table 4. Correlation matrix of element contents in crandallite-I (19 microprobe analyses).

	Al	P	S	Y	Sr	Ca	Fe	Ga	Ba	La	Ce	Pr	Nd	Sm	Gd	Dy	Er	Yb
P	-0.47	1.00																
S	0.14	0.40	1.00															
Y	0.03	0.36	0.11	1.00														
Sr	0.01	0.66	0.87	0.23	1.00													
Ca	-0.36	0.85	0.43	0.36	0.62	1.00												
Fe	-0.35	-0.35	-0.23	-0.43	-0.36	-0.25	1.00											
Ga	-0.30	0.07	-0.39	0.36	-0.27	-0.08	0.02	1.00										
Ba	-0.27	0.29	-0.12	-0.26	-0.01	0.09	-0.13	0.15	1.00									
La	-0.05	-0.45	-0.79	-0.17	-0.77	-0.63	0.13	0.54	0.06	1.00								
Ce	0.48	-0.17	0.45	0.18	0.27	0.05	-0.35	-0.53	-0.37	-0.55	1.00							
Pr	0.43	-0.68	-0.48	-0.45	-0.63	-0.82	0.05	-0.18	0.02	0.62	0.04	1.00						
Nd	0.24	-0.70	-0.62	-0.30	-0.78	-0.84	0.13	0.07	0.06	0.71	-0.03	0.90	1.00					
Sm	0.05	-0.58	-0.60	-0.02	-0.75	-0.58	0.20	0.26	-0.04	0.54	0.01	0.49	0.79	1.00				
Gd	-0.02	-0.34	-0.64	0.34	-0.60	-0.35	0.08	0.65	-0.21	0.64	-0.29	0.16	0.45	0.70	1.00			
Dy	0.11	-0.06	-0.29	0.53	-0.13	-0.11	-0.23	0.60	-0.18	0.38	-0.32	-0.08	0.04	0.21	0.69	1.00		
Er	0.17	0.36	0.47	0.00	0.56	0.30	0.00	-0.15	-0.03	-0.29	-0.14	-0.23	-0.43	-0.56	-0.45	-0.10	1.00	
Yb	0.12	0.04	0.24	0.22	0.11	-0.12	-0.24	-0.14	-0.07	-0.02	0.06	0.13	0.12	0.12	0.14	0.20	0.08	1.00
Pb	0.12	0.02	0.40	0.34	0.26	0.01	-0.41	-0.31	0.01	-0.44	0.70	-0.05	0.05	0.10	-0.17	-0.19	-0.21	0.33

Table 5. Correlation matrix of element contents in crandallite-II (23 microprobe analyses).

	Al	P	S	Y	Sr	Ca	Fe	Ga	Ba	La	Ce	Pr	Nd	Sm	Gd	Dy	Er	Yb
P	-0.46	1.00																
S	0.08	-0.69	1.00															
Y	0.09	0.03	-0.33	1.00														
Sr	0.13	-0.47	0.79	-0.40	1.00													
Ca	-0.37	0.83	-0.51	-0.41	-0.31	1.00												
Fe	-0.22	0.54	-0.70	0.06	-0.68	0.62	1.00											
Ga	0.19	-0.06	0.06	0.29	0.10	-0.16	0.01	1.00										
Ba	-0.19	0.64	-0.62	0.20	-0.38	0.53	0.55	0.28	1.00									
La	-0.09	-0.23	0.07	0.23	-0.17	-0.42	-0.16	0.07	-0.30	1.00								
Ce	-0.06	-0.44	0.41	0.00	0.20	-0.52	-0.50	-0.08	-0.67	0.82	1.00							
Pr	0.28	-0.16	-0.18	0.39	-0.29	-0.44	-0.17	-0.12	-0.39	0.59	0.46	1.00						
Nd	0.10	0.09	-0.39	0.70	-0.51	-0.35	-0.02	0.00	-0.14	0.52	0.39	0.78	1.00					
Sm	0.21	0.10	-0.46	0.70	-0.49	-0.34	-0.01	-0.02	-0.07	0.40	0.24	0.84	0.96	1.00				
Gd	0.19	0.15	-0.52	0.85	-0.54	-0.32	0.07	0.06	0.09	0.27	0.07	0.66	0.92	0.95	1.00			
Dy	0.12	0.13	-0.48	0.88	-0.57	-0.32	0.09	0.02	0.10	0.35	0.10	0.67	0.90	0.92	0.96	1.00		
Er	0.14	0.08	-0.36	0.52	-0.25	-0.02	0.32	0.28	0.30	-0.16	-0.25	-0.09	0.23	0.23	0.38	0.38	1.00	
Yb	0.27	0.03	-0.07	0.39	-0.25	-0.17	-0.05	0.32	0.30	0.17	0.00	0.16	0.27	0.32	0.34	0.37	-0.01	1.00
Pb	0.04	-0.74	0.79	0.04	0.33	-0.67	-0.49	0.06	-0.62	0.41	0.60	0.06	-0.04	-0.17	-0.20	-0.10	-0.17	0.13

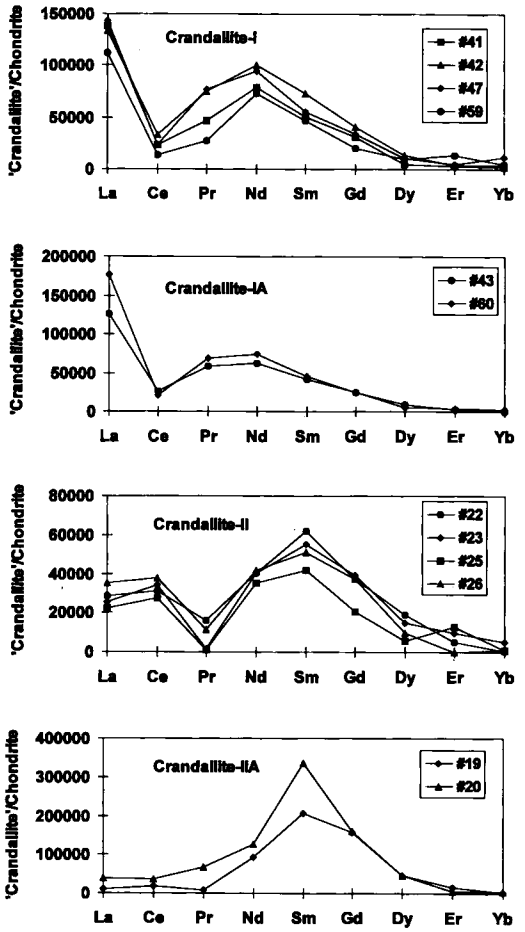

Fig. 6. Different types of chondrite-normalised (C_1) REE distribution in crandallites.

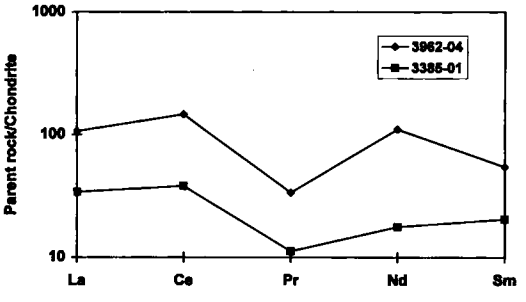

Fig. 7. Chondrite-normalized REE distribution pattern of silicate and carbonate parent rocks. Sample compositions are given in Table 1.

Four types of REE distribution in crandallite group minerals are distinguished from their chondrite-normalised patterns (Fig. 6). Of these, two types (crandallite-I and crandallite-IA) show a distinctive negative Ce anomaly, and a slight depletion of Pr can also be seen. The REE sum is high (9-15 wt.%). These varieties of crandallite were found only in sample 3962-14, which is free of organics (Table 1). It is typical that the type of the distribution pattern of crandallite-I does not result from crystal zoning.

Crandallite-II and crandallite-IIA have a sharp positive anomaly of Sm. With the exception of one case (point 20), a clear negative anomaly of Pr is observed as well. In the other analysed points, the content of Pr is below the detection limit, but the appearance of the patterns is the same. These two varieties of crandallite were found in sample 3346-08. They contain the lowest (1.5-8.2 wt.% in grain cores) and the highest (14-21 wt.% in grain rims) contents of REE respectively (as already stated the latter case can be termed florencite). It is notable, that within this sample all the analysed grains show the same REE distribution pattern. The difference between the core and the rim can be found only from the level of concentration of the elements. Also important is an enrichment of the sample with organic carbon. It forms 0.1-0.5 mm thick veinlets which carry crandallite and "leucoxene" mineralizations (Mordberg *et al.*, submitted). Although the bulk content of organics in the sample is not very high (Table 1), it is at least an order of magnitude higher than in other samples.

Crandallites I and II differ by the total amount of the REE (Table 3) the average of which is two times higher in crandallite-I. Crandallite-II is relatively enriched in S, Sr and Pb. Correlation analysis of element contents of crandallites (Tables 4, 5) also shows some differences between crandallites I and II. Thus, in crandallite-II, S correlates positively with both Pb and Sr, pointing to the presence of hinsdalite and svanbergite. In crandallite-I, S correlates positively with only Sr showing that Pb occurs in plumbogummite.

Data on REE in crandallites were compared with those in bulk parent rock and weathering profile (Table 1, Fig. 7-11). Of the three analysed samples from the parent rock, the first (7277-04) is composed of mainly silicate minerals such as feldspar, aegirine and riebeckite, while the second and the third are composed of silicates as well as carbonates (calcite and dolomite, samples 3385-01

and 7277-04 correspondingly). Chondrite-normalised REE patterns (La to Sm) of two samples show a negative Pr anomaly so that the appearance of this anomaly in crandallites can be explained by its inheritance from the parent rock (Fig. 7). The REE patterns of weathered rocks normalised to parent rock show their redistribution and accumulation during weathering with a more or less horizontal trend (Fig. 8, 9). Among different types of weathered rock, bauxite itself has the highest degree of REE accumulation. No substantial Ce depletion or Sm accumulation is observed. However, both Ce and Sm anomalies can be seen clearly on the REE patterns of crandallites normalised to bulk bauxite samples (Fig. 10, 11). This is evidence of Ce separation from crandallite-I and Sm accumulation in crandallite-II during their formation.

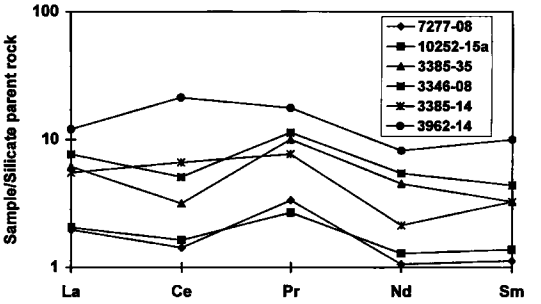

Fig. 8. REE distribution patterns of weathered rocks normalized to silicate parent rock. Sample compositions are given in Table 1.

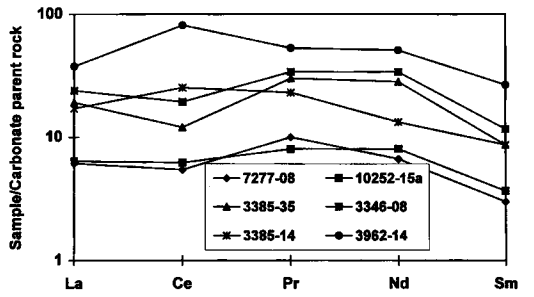

Fig. 9. REE distribution patterns of weathered rocks normalized to carbonate parent rock. Sample compositions are given in Table 1.

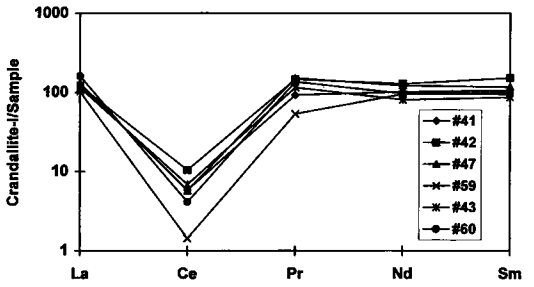

Fig. 10. REE distribution pattern of crandallite-I normalized to bulk sample.

Discussion

REE mobilisation and migration

Release of the REE during weathering occurred according to the dissolution rates of parent rock minerals. Dissolution of rock-forming calcite, dolomite and K-feldspar should have provided neutral to alkaline media with the carbonate ion dominating in solution. Locally, sulphate and phosphate ions could play a more important role due to dissolution of sulphides and P-bearing minerals such as apatite.

For light REE (LREE), the dominant carbonate complex is $[LREE(CO_3)]^{1+}$, while for heavy REE (HREE) a complex such as $[HREE(CO_3)_2]^{1-}$ dominates in solution (Cantrell & Byrne, 1987). Among inorganic complexes, carbonate complexes are more frequent in the pH range 7 to 9; above pH 9 hydroxyl complexes prevail, and below pH 7 REE^{3+} ions dominate, while the role of sulphate and halide complexes is subordinated (deBaar *et al.*, 1988; Lee & Byrne, 1992). An increase of pH decreases the role of REE^{3+} ions, especially for HREE. In slightly alkaline environments (pH = 8-9), LREE prevail as carbonate complexes, while for HREE phosphate complexes are more typical.

The presence of organic ligands substantially changes existing REE complexes. Thus, oxalate complexes seem to prevail within the pH interval 4 to 8; at lower pH REE^{3+} ions are more widespread and sulphate complexes such as $[REESO_4]^{1+}$ may appear, while an increase of pH leads to an increase in the role of carbonate and phosphate complexes such as $[REEPO_4]^{2+}$ or $[REE(PO_4)_2]^{3-}$ (Wood, 1993). It should be noted that all the above estimations are based on some assumptions, such as equal activity of all species, comparably low concentration of REE and absence of ions of other metals in the solution.

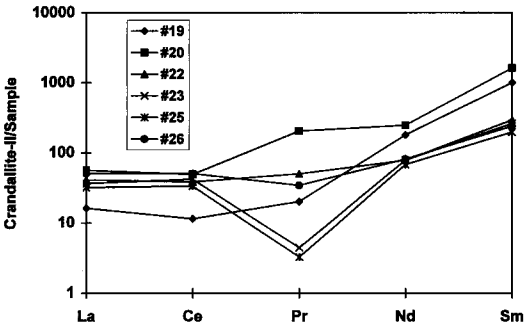

Fig. 11. REE distribution pattern of crandallite-II normalized to bulk sample.

Crystal chemistry of crandallites

Crandallite and the other Al- and Fe-phosphates and -arsenates belong to the alunite family. According to recent generalisations (Gaines *et al.*, 1997), three groups can be distinguished, namely crandallite, florencite and beudantite. The simplified general formula which fits all end members can be written as

$$AB_3(XO_4)_2(OH)_6H_{0\text{ or }1}$$

where A = Ca, Ba, Sr, Pb, Bi, REE, Th, □; B = Al, Fe^{3+} and Ga; and X = P, As, S, Si and C. The presence of an extra H depends on the cation charge in the A- and X-sites.

In crandallites, A-site cations occur in 12-fold, B-site in 6-fold, and X-site in tetrahedral coordination (Kato, 1971, 1990; Blount, 1974; Radoslovich, 1982). Florencite, which has trivalent REE cations in the A-site (Kato, 1990), does not require an extra proton, similarly for the S-bearing minerals (Kato, 1971). The crystal structure and exact formula of crandallite $CaAl_3[PO_3(O_{1/2}OH_{1/2})]_2(OH)_6$ were determined by Blount (1974), who found that an extra proton was bonded to both apical oxygens of PO_4 tetrahedra. Later on, Radoslovich (1982) found that the formula of the Ba-analogue gorceixite was $BaAl_3(PO_4)(PO_3OH)(OH)_6$, because of O replacement by OH in only one of two PO_4 tetrahedra. He also supposed that the same could be observed in goyazite and plumbogummite. This is based on the fact that although the A-site cation occurs in 12-fold coordination, the Ca-ion is relatively small, and actually coordinates with only eight ions. Since Ba-, Sr- and Pb-ions are sufficiently larger than Ca, they coordinate with all twelve ions. This is confirmed by linear correlation between cell constants and ion sizes for the elements from Ba^{2+} (the largest) to Ca^{2+} and Ce^{3+}, while smaller ions deviate somewhat from this dependance (Schwab *et al.*, 1990). The distance between apical oxygens of PO_4 tetrahedra in gorceixite is higher; therefore, an extra proton can be bonded with only one of the apical oxygens. This changes the space group of gorceixite to Cm (Radoslovich, 1982). As S frequently occurs in the X-site, the problem of order - disorder in this site can also affect the nomenclature of crandallites (Sejkora *et al.*, 1998): an ordered PO_4 and SO_4 distribution was found only for corkite $PbFe^{3+}{}_3(PO_4)(SO_4)(OH)_6$ (Giusepetti & Tardini, 1987).

Taking into account these details of crystal structure and analytical data, we can give the formula of analysed crandallites from the Schugorsk deposit as

$$A^{2+}{}_{1-x}A^{3+}{}_xB_3[X^{5+}O_4]_{1+x}[(X^{5+}O_3OH),(X^{6+}O_4)]_{1-x}(OH)_6$$

where x may vary from 0 to 1; A^{2+} = Ca, Sr, Ba, Pb and Bi, A^{3+} = Y and REE, B = Al, Ga and Fe^{3+}, X^{5+} = P and V, and X^{6+} = S. This follows the idea of Somina & Bulah (1966) and Sejkora *et al.* (1998) with the specification of A- and X-sites.

Thermodynamic properties of crandallites

Consideration of thermodynamic properties of pure synthetic crandallites on the basis of Gibbs free energies shows their general agreement with crystal chemistry data. Thus, the stability of florencites against gibbsite increases in the sequence HREE < Gd < Eu < Pr < Sm < Ce < Nd < La for trivalent ions (Schwab *et al.*, 1993). Among the pure Al-phosphate species of crandallite type with divalent A-site metals, thermodynamic stability (also against gibbsite) increases in sequence $Pb^{2+} > Sr^{2+} > Ba^{2+} > Ca^{2+}$ that suggests better fitting of Pb- and Sr-ion sizes to the 12-fold coordinated site (Schwab *et al.*, 1993). Although in our case crandallites exist in association with boehmite, the sequence of stabilities should be similar, since it is related to crystal chemistry, and particularly, to ion sizes (Schwab *et al.*, 1990, 1993).

An approach to the estimation of conditions of crandallite formation can be made from data on thermodynamic stabilities of Pb phosphates. At reasonable activities of Al^{3+}, Pb^{2+}, carbonate and

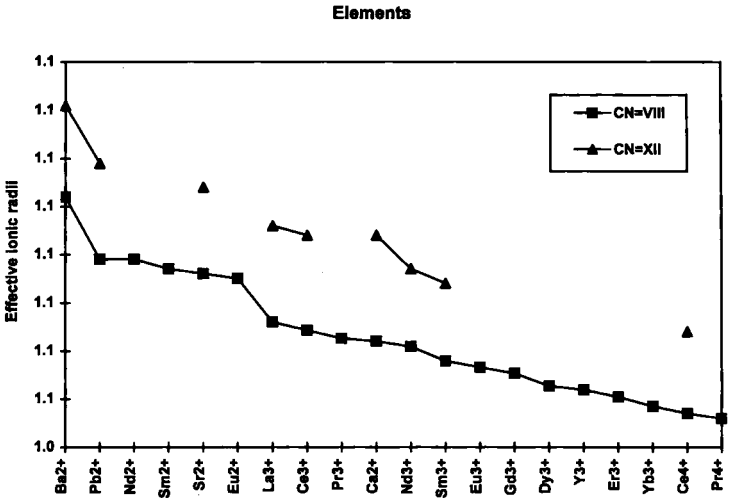

Fig. 12. Effective ionic radii (Å) of REE and other elements in 8- and 12-fold coordination (after Shannon, 1976).

sulphate ions, plumbogummite $PbAl_3(PO_4)_2H(OH)_6$ and hinsdalite $PbAl_3(PO_4)(SO_4)(OH)_6$ are stable in alkaline environments, the former being stable at higher phosphate ion activity, and the latter at lower phosphate ion activity (Nriagu, 1984b). This may be important for understanding the conditions of crandallite-II formation. High contents and positive correlation of Pb and S in crandallite-II point to the existence of hinsdalite cells, and therefore, to relatively low activity of PO_4^{3-} or HPO_4^{2-}.

REE oxidation states

Although the REE exist in nature mainly in trivalent form, tetravalent Ce and divalent Eu are also well known (Henderson, 1996). At 25 °C, CeO_2 is a stable form of Ce^{4+} within a wide range of pH and Eh, especially in alkaline media (Brookins, 1989). Therefore, oxidizing conditions of weathering commonly lead to the formation of cerianite CeO_2 (Braun *et al.*, 1990, 1998; Mongelli, 1997). The present patterns (crandallite-I and IA) look very similar to that which can be calculated from an analysis of 'REE-bearing goyazite' from a Yugoslavian karst bauxite deposit given by Maksimović & Panto (1985). The same REE distribution (La to Sm) was found in apatite-derived florencite from a weathering profile over granites in New South Wales, Australia (Banfield & Eggleton, 1989). These patterns represent a negative Ce anomaly and can be explained by strong oxidising conditions of weathering, which should have oxidised Ce to the tetravalent state. Cerianite itself has not been recorded within the studied profile; however, indirect evidence that Ce^{4+} exists there is its accumulation in 'leucoxene' and a Th-rich unknown phosphate (Mordberg *et al.*, submitted) where it may replace Ti^{4+} or Th^{4+} accordingly.

The observed patterns II and IIA are quite unusual and need consideration of REE oxidation states because of the Sm anomaly. A similar pattern with a slight positive Sm anomaly was also observed in crandallite from P-rich laterite profile of the Lam-Lam deposit, Senegal (Bonnot-Courtois & Flicoteaux, 1989). Cesbron (1986) believes that Sm^{2+}, as well as Eu^{2+}, may be sufficiently stable in aqueous solutions. This opinion is supported by consideration of thermochemical data. At temperatures above 250 °C the dominant form of Eu is likely to be divalent, while at low temperatures (25 °C), Eu^{3+} dominates in solution (Sverjensky, 1984). Within this temperature interval, both forms may be present. Divalent Eu can be expected in low-temperature aqueous solution together with SO_4^{2-} in alkaline media (pH > 9) and low oxygen fugacity (Sverjensky, 1984). Calculations also show, that Sm and Yb have a similar trend of equilibria between divalent and trivalent ions (Wood, 1990). For the most widespread geological environments, Sm^{2+} dominates in solution at temperatures above 400 °C; however, under extremely reducing and/or alkaline conditions it may appear at lower temperatures (Wood, 1990). There is also evidence that Sm^{2+} occurs in natural fluorite as a result of irradiation damage (Bill & Calas, 1978).

The diadochy of REE to other elements is crucially dependent on ionic radii. For the REE and other A-site cations, these data are given in Fig. 12. Although not all radii of REE are known for 12-fold coordination, some conclusions can be made from the existing data. One can believe that, with respect to the REE, this coordination is restricted to large cations (Cesbron, 1986). The three known varieties of florencite (florencite-(La), florencite-(Ce) and florencite-(Nd)) (Burt, 1989) seem to confirm this opinion, as well as lattice constant dependences and thermodynamic stabilities (Schwab *et al.*, 1990, 1993).

The ionic radius of Sm^{3+} is relatively close to that of Ca^{2+}, but much smaller than those of Pb^{2+} and Sr^{2+}. However, the ionic radius of Sm^{2+} in 8-fold coordination is very close to those of Pb^{2+} and Sr^{2+} (Fig. 12). For 12-fold coordination, the ionic radius of Sm^{2+} is not determined, but from the observed patterns, we may suppose that it is also very similar to Pb^{2+} and Sr^{2+}. The structure of crandallites bearing Sm^{3+} and other relatively small REE ions could be sufficiently stabilised by the presence of large Pb^{2+} and Sr^{2+} ions (Schwab *et al.*, 1993). However, this cannot explain the appearance of the Sm anomaly in crandallite-II, as it does not exist in the parent rock or bulk weathered samples.

As was already discussed above, reduction of Sm^{3+} to Sm^{2+} could occur under strongly reducing conditions which played an important role in the development of the Schugorsk deposit. Total dissolution of hematite and removal of Fe are evidence for this, as well as the formation of sulphide minerals such as galena, pyrite and sphalerite (Likhachev, 1993; Mordberg *et al.*, submitted). The role of organics seems to be quite important, but needs a detailed study. However, this process may be related not only with low-temperature diagenetic transformation, but also with superimposed hydrothermal alteration (Mordberg, 1997; Mordberg *et al.*, submitted).

Crandallite formation

The sources of the REE in the parent rock were carbonates (calcite and dolomite) and feldspar, as well as some REE-bearing minerals such as bastnaesite, monazite and xenotime (Mordberg *et al.*, submitted). Although the background level of the REE in carbonates and feldspars is low, the volume of rock dissolved to form the bauxite deposit was high enough to release significant amounts of these elements. Following the dissolution of primary rock minerals, REE released in this weathering process could exist in solution as carbonate complexes such as $[LREE(CO_3)]^+$ or $[HREE-(CO_3)_2]^{1-}$. Locally, they might also occur as REE^{3+} and $REE(SO_4)^{2+}$ (acidic environment), $REE(P_2O_7)^-$ (alkaline environment) and organic complexes (nearly neutral environment). The formation of crandallite group minerals took place during the weathering process. The complicated chemical distribution in individual crandallite group mineral crystals is directly related to the rates of dissolution of minerals from the parent rock, the source of P being primary apatite. Two methods of crandallite formation have previously been described: a direct replacement of apatite by attack of the weathering solution (Viellard *et al.*, 1979) and formation through apatite dissolution and subsequent precipitation (Schwab *et al.*, 1989). Both partial dissolution and direct alteration must have taken place in the Timan occurrence and is illustrated in Fig. 3 and 4: it seems that crandallite mineralization in the centre of the area (Fig. 3) may have inherited the shape of, initially, an apatite crystal. Deep weathering destroyed the crystal, and its remains altered into Ca-rich crandallite. This can be confirmed by the fact that Ca-crandallite itself forms cores of the grains (Fig. 4). The formation of Sr-, Pb- and REE-rich rims took place later through supply of these elements from the weathering solution. The dissolved part of P could precipitate within a short distance from the apatite crystal, also with the formation of crandallite group minerals. This may explain the existence of small individual grains around the zone of crandallite mineralization (Fig. 3).

In a karstic environment, REE usually accumulate within a comparatively thin layer above the footwall. They preferentially form carbonate minerals of the bastnaesite group (Maksimović & Pantó, 1996). In laterites over P-rich rocks, crandallites form a distinctive layer together with other Al-phosphates (Schwab *et al.*, 1989). Such a layer may form even in karstic environment, if the parent rock is enriched in P-minerals such as apatite (Mordberg, 1999). However, the studied profile cannot be referred to as exclusively karstic or lateritic due to the composition of parent rock and selective weathering. Only disseminated crandallite mineralization was found.

Not too many data are known on REE distribution in crandallites from weathering profiles,

although they are relatively widespread. A mineral with a composition intermediate between Nd-florencite, goyazite and crandallite occurs in the bauxite deposit of Vlasenica, Yugoslavia (Maksimović & Pantó, 1985). Gorceixite and florencite were recorded in the Lohrheim kaolinite deposit, Germany (Dill *et al.*, 1995). Minerals of the crandallite group, such as goyazite, gorceixite and florencite, have been observed in bauxitic kaolins of NE Sudan (Wipki, 1995; Germann *et al.*, 1995; Schwarz & Germann, 1999). Florencite and crandallite are typical of weathering profiles over carbonatites (Slukin *et al.*, 1989; Wall *et al.*, 1996). Morteani & Preinfalk (1996) believe that gorceixite is the main concentrator of the REE in laterite over alkaline rocks of Araxá and Catalão (Brazil). Gorceixite was also found in a weathering profile over apatite-rich carbonatite of Juquiá (Brazil); there, it shows a specific distribution of the REE with the enrichment in La, Ce and especially Nd, and close chondrite-normalised values for the elements from Sm to Yb (Walter *et al.*, 1995). The contents of the REE in that gorceixite are very low (0.00n-0.n wt.%), presumably because of the very high ionic radius of Ba, that restricts the isomorphic capacity of the mineral with respect to the REE. Therefore, strong accumulation of the REE in gorceixite is doubtful. The data presented, as well as the observation made, show that the number of known occurrences of REE-crandallites in weathering profiles is high, and the distribution of the REE is different in them. These patterns can be used for the explanation of the formation of one or other mineral assemblage of bauxite or laterite and for the determination of geological and geochemical conditions of deep weathering.

Conclusions

Summarizing the results and discussion, we distinguish two generations of crandallites within the Schugorsk bauxite deposit. The first one formed under oxidizing conditions (positive Eh values) in a neutral to slightly alkaline environment. Oxidising conditions were responsible for the development of a negative Ce anomaly. Extra Ce was distributed among minerals, which carry tetravalent ions, such as Ti ('leucoxene') or Th (unknown Th-rich phosphate). It is supposed, that reducing conditions (negative Eh values, more alkaline media with pH 8-9 and low oxygen fugacity) led to the formation of Sm-rich crandallite-II where Sm^{3+} might have been reduced to Sm^{2+}. This may replace Sr^{2+} and/or Pb^{2+} and form the cell identical to that of svanbergite and hinsdallite.

Crandallite group minerals from the Schugorsk bauxite deposit have a very complicated composition and clear zonal distribution of cations in all sites, that reflects the history of their formation. The core is composed of mainly crandallite itself with other elements as admixtures. The rim is enriched in Sr, Pb, S and REE representing the occurrence of goyazite-svanbergite, plumbogummite-hinsdallite and florencite. Weathering of apatite from the parent rock resulted in formation of crandallite both *in situ* (direct alteration) and within a small distance through its dissolution and following P and Ca precipitation due to high Al activity in the weathering solution.

The results of the present study and comparison with existing data show that crandallite group minerals have a broad distribution among bauxitic and lateritic profiles of different origins and may represent quite different patterns of the REE whose high sensitivity to changes in Eh-pH makes them quite important for the specification of conditions of deep weathering.

Acknowledgement: The research described has been supported by scholarship from Alfred Toepfer Foundation F.V.S. (Hamburg) and Postdoctoral Fellowship from NATO/Royal Society for Dr. Leonid Mordberg. The authors are very grateful to Dr. C. T. Williams and Mr. J. Spratt for the performance of microprobe analyses and X-ray mapping. The comments of Prof. C. Gomes and an anonymous referee contributed much to our understanding of crandallite formation.

References

Ansheles, O.M. & Vlodavets, N.I. (1927): Strontium mineral from Tikhvin bauxites. *Zap. Vses. Min. Obshch.*, **56**, 53-60 (in Russian).

Banfield, J.F. & Eggleton, R.A. (1989): Apatite replacement and rare earth mobilization, fractionation, and fixation during weathering. *Clays Clay Min.*, **37**, 113-127.

Bárdossy, Gy. (1982): Karst bauxites. Bauxite deposits on carbonate rocks. Elsevier, Amsterdam, 441 p.

Beneslavsky, S.I. (1974): Mineralogy of bauxites. 2nd Ed., Nedra, Moscow, 168 p. (in Russian).

Bill, H. & Calas, G. (1978): Colour centres, associated rare-earth ions and the origin of coloration in natural fluorites. *Phys. Chem. Minerals*, **3**, 117 - 131.

Blount, A.M. (1974): The crystal structure of crandallite. *Am. Mineral.*, **59**, 41-47.

Bonnot-Courtois, C. & Flicoteaux, R. (1989): Distribution of rare-earth and some trace elements in Tertiary phosphorites from the Senegal Basin and their weathering products. *Chem. Geol.*, **75**, 311-328.

Braun, J.-J., Pagel, M., Muller, J.P., Bilong, P., Michard, A., Guillet, B. (1990): Cerium anomalies in lateritic profiles. *Geochim. Cosmochim. Acta*, **54**, 781-795.

Braun, J.-J., Viers, J., Dupré, M., Ndam, J., Muller, J.-P. (1998): Solid/liquid REE fractionation in the lateritic system of Goyom, East Cameroon: The implication for the present dynamics of the soil covers of the humid tropical regions. *Geochim. Cosmochim. Acta,* **62**, 273-299.

Brookins, D.G. (1989): Aqueous geochemistry of rare earth elements. *Rev. Mineral.*, **21**, 201-226.

Bulgakova, A.P. (1967): Epigenetic svanbergite in the weathering crust of Lebedinsk deposit, KMA. *Zap. Vses. Min. Obshch.*, **96**, 342-345 (in Russian).

Burt, D.M. (1989): Compositional and phase relations among rare earth minerals. *Rev. Mineral.*, **21**, 259-307.

Bushinsky, G.I. (1975): Geology of bauxites. 2nd Ed., Nedra, Moscow, 368 p. (in Russian).

Cantrell, K.J. & Byrne, R.H. (1987): Rare earth element complexation by carbonate and oxalate ions. *Geochim. Cosmochim. Acta*, **51**, 597-606.

Cesbron, F.P. (1986): Mineralogy of the Rare-Earth Elements. *in* "Lanthanides, Tantalum and Niobium", P. Möller, P. Černý, & F. Saupé, eds. Springer-Verlag, Berlin, 3-26.

deBaar, H.J.W., German, C.R., Eldergield, H., Van Gaans, P. (1988): Rare element distributions in anoxic waters of the Cariaco Trench. *Geochim. Cosmochim. Acta*, **52**, 1203-1220.

Dill, H.G., Fricke, A., Henning, K.H. (1995): The origin of Ba-bearing and REE-bearing aluminium-phosphate-sulphate minerals from the Lohrheim kaolinitic clay deposit (Rheinisches Schiefergebirge, Germany). *Appl. Clay Sci.*, **10**, 231-245.

Gaines, R.V., Skinner, H.C.W., Foord, E.E., Mason, B., Rosenzweig, A. (1997): Dana's new mineralogy. The system of mineralogy of James Dwight Dana and Edward Salisbury Dana. John Wiley & sons inc., NY, 1819 p.

Germann, K., Fischer, K., Schwarz, T., Wipki, M. (1995): Distribution and origin of bauxitic laterites in NE-Africa. *in* "Mineral Deposits: from their origin to their environmental impacts", J. Pasava, B. Kribek & K. Zak, eds. Balkema, Rotterdam, 577-580.

Giusepetti, G. & Tardini, C. (1987): Corkite, $PbFe_3(SO_4)(PO_4)(OH)_6$, its crystal structure and order arrangement of the tetrahedral cations. *N. Jb. Miner. Mh.*, **1987**, 71-81.

Gomes, C.S.F. (1968): On a Sr and Al basic phosphate-sulphate close to svanbergite occurring in a Portuguese bauxitic clay. *Mem. Not. Mus. Lab. Min. Geol. Universidade de Coimbra*, **66**, 3-13.

Henderson, P. (1996): The rare earth elements: introduction and review. *in* "Rare Earth Minerals. Chemistry, origin and ore deposits", P. Jones, F. Wall & C.T. Williams, eds. Chapman & Hall, London, 1-20.

Kato, T. (1971): The crystal structures of goyazite and woodhouseite. *N. Jb. Miner. Mh.*, **1971**, 241–247.

– (1990): The crystal structure of florencite. *N. Jb. Miner. Mh.*, **1990**, 227-231.

Krumb, J.H. (1998): Bedingungen, Prozesse und Stoffbilanz der Kaolinisierung - das Beispiel der Lagerstätten Sachsens. Bodoni, Berlin, 224 p.

Lee, J.H. & Byrne, R.H. (1992): Examination of comparative rare earth element complexation behaviour using linear free-energy relationships. *Geochim. Cosmochim. Acta,* **56**, 1127-1137.

Likhachev, V.V. (1993): Rare-metal bauxite-bearing weathering crust of the Middle Timan. Komi nauchny tsentr UrO RAN, Syktyvkar, 224 p. (in Russian).

Lukanina, M.I. (1959): Svanbergite in bauxites of Kamenski District in the Middle Ural. *Zap. Vses. Min. Obshch.*, **88**, 586-591 (in Russian).

Makarov, V.N. (1967): Mineral from svanbergite series in the weathering crust of Jakovlevsk deposit, KMA. *Zap. Vses. Min. Obshch.*, **96**, 342-345 (in Russian).

Maksimović, Z. & Pantó, Gy. (1985): Neodymian goyazite in the bauxite deposit of Vlasenica, Yugoslavia. *Tschermaks Mineral. Petrogr. Mitteilungen*, **34**, 159-165.

– – (1996): Authigenic rare earth minerals in karst-bauxites and karstic nickel deposits. *in* "Rare Earth Minerals. Chemistry, origin and ore deposits", P. Jones, F. Wall & C.T. Williams, eds. Chapman & Hall, London, 257-279.

Mongelli, G. (1997): Ce-anomalies in the textural components of Upper Cretaceous karst bauxites from the Apulian carbonate platform (southern Italy). *Chemical Geol.*, **140**, 69-79.

Mordberg, L.E. (1996): Geochemistry of trace elements in Paleozoic bauxite profiles in northern Russia. *J. Geochem. Explor.*, **57**, 187-199.

– (1997): Geology, geochemistry and origin of the Schugorsk bauxite deposit, Middle Timan, Russia. *Travaux ICSOBA*, **24**, 35-42.

– (1999): Geochemical evolution of a Devonian diaspore-crandallite-svanbergite-bearing weathering profile in the Middle Timan, Russia. *J. Geochem. Explor.*, **66**, 353-361.

Mordberg, L.E. & Spratt, J. (1998): Alteration of zircons: the evidence of Zr mobility during bauxitic weathering. *Mineral. Mag.*, **62A**, 1021-1022.

Morteani, G. & Preinfalk, C. (1996): REE distribution and REE carriers in laterites formed on the alkaline complex of Araxá and Catalão (Brazil). *in* "Rare Earth Minerals. Chemistry, origin and ore deposits", P. Jones, F. Wall & C.T. Williams, eds. Chapman & Hall, London, 227-255.

Nriagu, J.O. (1984a): Phosphate minerals: their properties and general modes of occurrence. *in* "Phos-

phate minerals", J.O. Nriagu & P.B. Moore, eds. Springer-Verlag, Berlin, 1-136.

– (1984b): Formation and stability of base metal phosphates in soils and sediments. *in* "Phosphate minerals", J.O. Nriagu & P.B. Moore, eds. Springer-Verlag, Berlin, 318-329.

Radoslovich, E. W. (1982): Refinement of gorceixite structure in Cm. *N. Jb. Miner. Mh.*, **1982**, 446-464.

Rasmussen, B. (1996): Early-diagenetic REE-phosphate minerals (florencite, gorceixite, crandallite and xenotime) in marine sandstones: a major sink for oceanic phosphorus. *Am. J. Sci.*, **296**, 601-632.

Schwab, R.G., Costa, M. L. da, Oliveira, N.P. de, (1983): Über die Entwicklung von Bauxiten und Phosphat-Lateriten der Region Gurupi, Nordbrasilien. *Zentralbl. Geol. Paläont.*, Teil I, 563-580.

Schwab, R.G., Götz, C., Herold, H., Oliveira, N.P. de (1990): Compounds of crandallite type: Synthesis and properties of pure Rare Earth Element-phosphates. *N. Jb. Miner. Mh.*, **1990**, 241-254.

Schwab, R.G., Herold, H., Costa, M. L. da, Oliveira, N.P. de (1989): The formation of aluminous phosphates through lateritic weathering of rocks. *in* "Weathering; its products and deposits", Vol. **2**, A. Barto-Kyriakidis, ed. Theophrastus Publishing & Proprietary Co., S.A. (Ltd.), Athens, 369-386.

Schwab, R.G., Herold, H., Götz, C., Oliveira, N.P. de (1993): Compounds of crandallite type: Thermodynamic properties of Ca-, Sr-, Ba-, Pb-, La-, Ce- to Gd-phosphates and -arsenates. *N. Jb. Miner. Mh.*, **1993**, 551-568.

Schwarz, T. & Germann, K. (1999): Weathering surfaces, laterite-derived sediments and associated mineral deposits in north-east Africa. *Spec. Publ. Int. Ass. Sediment.*, **27**, 367-390.

Sejkora, J., Cejka, J., Novotná, M., Ederová, J. (1998): Minerals of the plumbogummite-philipsbornite series from Moldava deposit, Krušné hory Mts., Czech Republic. *N. Jb. Min. Mh.*, **1998**, 145-163.

Shannon, P.D. (1976): Revised effective radii and systematic studies of interatomic distances in halides and chalcogenides. *Acta Cryst., Sect. A*, **32**, 751-767.

Slukin, A.D., Arapova, G.A., Zvezdinskaya, L.V., Tsvetkova, M.V., Lapin, A.V. (1989): Mineralogy and geochemistry of laterized carbonatites of the USSR. *in* "Weathering; its products and deposits", Vol. **2**, A. Barto-Kyriakidis, ed. Theophrastus Publishing & Proprietary Co., S.A. (Ltd.), Athens, 171-189.

Somina, M.J. & Bulah, A.G. (1966): Florencite from the Eastern Sayan carbonatites and some questions of chemistry of the crandallite group minerals. *Zap. Vses. Min. Obshch.*, **95**, 537-550 (in Russian).

Sverjensky, D.A. (1984): Europium redox equilibria in aqueous solution. *Earth Planet. Sci. Lett.*, **67**, 70-78.

Viellard, Ph., Tardy, Y., Nahon, D. (1979): Stability fields of clays and aluminium phosphates: paragenesis in lateritic weathering of argillaceous phosphatic sediments. *Am. Mineral.*, **64**, 626-634.

Wall, F., Williams, C.T., Wooley, A.R., Nasraoui, M. (1996): Pyrochlore from weathered carbonatite at Lueshe, Zaire. *Mineral. Mag.*, **60**, 731-750.

Walter, A.-V., Nahon, D., Flicoteaux, R., Girard, J.P., Melfi, A. (1995): Behaviour of major and trace elements and fractionation of REE under tropical weathering of a typical apatite-rich carbonatite from Brazil. *Earth Planet. Sci. Letters*, **136**, 591-602.

Williams, C.T. (1996): Analysis of rare earth minerals. *in* "Rare Earth Minerals. Chemistry, origin and ore deposits", P. Jones, F. Wall & C.T. Williams, eds. Chapman & Hall, London, 327-348.

Wipki, M. (1995): Eigenschaften, Verbreitung und Entstehung von Kaolinlagerstätten im Nordsudan. Köster, Berlin, 213 p.

Wood, S.A. (1990): The aqueous geochemistry of the rare-earth elements and yttrium 2. Theoretical predictions of speciation in hydrothermal solutions to 350 °C at saturation water vapor pressure. *Chemical Geol.*, **88**, 99-125.

– (1993): The aqueous geochemistry of the rare-earth elements: Critical stability constants for complexes with simple carboxylic acids at 25 °C and 1 bar and their application to nuclear waste management. *Engineering Geol.*, **34**, 229-259.

Received 25 June 1999
Modified version received 16 February 2000
Accepted 15 June 2000